

Seasonal climate summary southern hemisphere (spring 2002): the El Niño reaches maturity and dry conditions dominate Australia

Andrew B. Watkins

National Climate Centre, Bureau of Meteorology, Australia

(Manuscript received July 2003)

Atmospheric and oceanic conditions in the southern hemisphere are reviewed for the 2002 austral spring season. Particular emphasis is given to the Australian and Pacific regions. The El Niño event that emerged in the equatorial Pacific Ocean during autumn and winter reached its peak late in the spring of 2002. Ocean surface and sub surface temperatures in the tropical Pacific remained well above normal throughout the period, driving changes in the overlying Walker circulation and hence modifying many atmospheric parameters, including cloudiness, winds and surface pressures. Teleconnections ensured that such changes induced remote impacts throughout the southern hemisphere. The El Niño event, its growth earlier in the year, the start of its decay late in spring as well as its broadscale modification of the southern hemisphere atmosphere, was highly consistent with theoretically expected behaviour. For Australia, widespread dry conditions dominated the country, with low cloud amounts and a southwards shift in the westerlies; both consistent with the impacts of an El Niño in the Pacific. The generally low rainfall during spring was further exacerbated by very high maximum temperatures and hence greatly increased evaporation, consolidating the event as one of the worst Australian droughts in recorded history. Over the Antarctic, the springtime ozone hole expanded to its smallest size since 1988, reaching only 19 million square kilometres before splitting into two regions.

Introduction

The El Niño – Southern Oscillation (ENSO) maintained its warm state through the austral spring of 2002, however the Southern Oscillation Index (SOI)

remained only weakly negative, with values of -7.6 , -7.4 and -6.0 for September, October and November respectively. This resulted in a seasonal mean SOI of -7.0 , an increase of 1.5 since the winter season (Jones 2003). The SOI for spring (arguably) did not reflect the full strength of the event. The Multivariate ENSO Index (MEI), however, remained closer to one standard deviation throughout the spring. Sea-surface temperature (SST) values remained positive along the

Corresponding author address: Andrew B. Watkins, National Climate Centre, Bureau of Meteorology, GPO Box 1289K Melbourne, Vic. 3001, Australia.
Email: A.Watkins@BoM.GOV.AU

equator east of the date-line, with anomaly values generally above $+1.0^{\circ}\text{C}$. Subsurface values also remained warmer than normal in the central and eastern equatorial Pacific, whilst later in the season, cooler than normal waters became apparent in the western equatorial Pacific. This not only signalled the strongest west to east subsurface gradient of the event, and hence arguably the event's peak, but was also the first sign of the eventual breakdown of the El Niño itself. The atmospheric response was highlighted by the outgoing long wave radiation anomalies, which showed significant negative values during spring implying increased high cloud along the equator particularly near the date-line.

Over the Australian region, anticyclonic circulation in the low levels highlighted the general subsidence and hence reduced cloudiness which resulted in very much below average rainfall over most of the eastern half of the continent. The Australia-wide rainfall accumulation for spring was the fifth lowest since 1900. Maximum temperatures were well above average, with the Australia-wide value being the hottest on record in the post-1950 period by a considerable margin. Minimum temperatures tended to be near the long-term mean, however they were considerably warmer than during previous El Niño related droughts. Such patterns in temperature and rainfall generally reflect what may have been expected during a warm ENSO state (Jones and Trewin 2000), however the magnitudes of the anomalies were exceptionally strong.

Data

The main sources of information used for this summary were the *Climate Monitoring Bulletin* (Bureau of Meteorology, Melbourne, Australia) and the *Climate Diagnostics Bulletin* (Climate Prediction Center, Washington D.C., USA). Data sources are given in the Appendix.

Pacific Basin climate indices

The Southern Oscillation Index (SOI)*

After the austral winter of 2002 maintained the trend of negative seasonal mean values of the SOI (-7.8 and -9.5 for autumn and winter respectively) (Fawcett and Trewin 2003; Jones 2003), spring 2002 continued to display moderately negative values of the SOI.

*The SOI used here is ten times the monthly anomaly of the difference in mean sea-level pressure between Tahiti and Darwin, divided by the standard deviation of that difference for the relevant month, based on the period 1933-92.

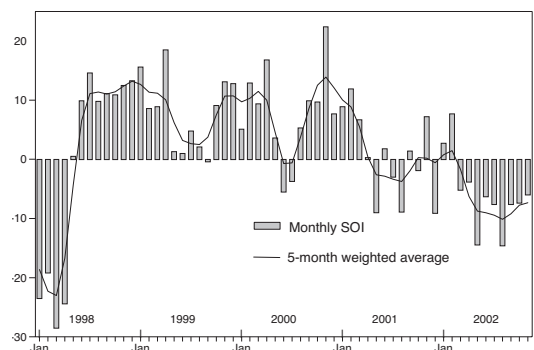
September, October and November 2002 SOI values were -7.6 , -7.4 and -6.0 respectively, resulting in a mean value of the SOI of -7.0 for spring 2002 (see Fig. 1), suggesting that SOI values were always within one standard deviation of the mean. (The Troup SOI has a standard deviation of 10.) Raw Tahiti minus Darwin values, from which the SOI is derived, only remained below one standard deviation during early to mid September, before returning to within one standard deviation until late in November, when again they fell below the normal range.

For the first two months of spring 2002 the negative values of the SOI index were mostly derived from negative Tahiti mean sea-level pressure (MSLP) anomalies, which were around 1 hPa below their long-term mean through September and October, while Darwin experienced near normal MSLP anomalies during this time. However, in November, Tahiti anomalies returned to near normal, while Darwin experienced MSLP anomalies averaging 1.1 hPa above normal.

These weakly negative values failed to truly reflect the full coupled ocean atmosphere state, which was undoubtedly warm at this time, having reached this state during winter (Jones 2003).

The fully coupled warm state of the equatorial Pacific was better highlighted by the Climate Diagnostics Center (CDC) Multivariate ENSO Index (MEI) (Wolter and Timlin 1993, 1998), an index derived from a number of atmospheric and oceanic parameters typically associated with El Niño and La Niña, with negative values indicating cooler conditions and positive values indicating warmer conditions. The MEI values remained close to one standard deviation throughout the spring, with values ranked between 42 and 44 out of 53 years. (An MEI ranking of 43 to 53 is considered to be an El Niño event.)

Fig. 1 Southern Oscillation Index, January 1998 to November 2002 inclusive. Means and standard deviations based on the period 1933-92.



Outgoing long wave radiation

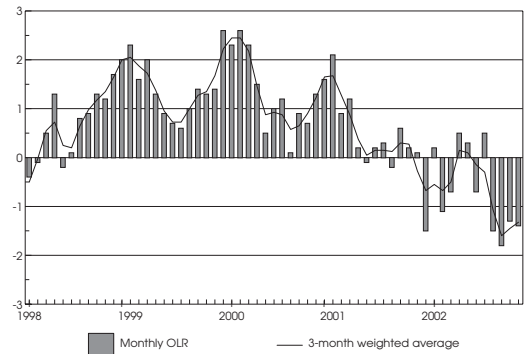
The time series from January 1998 to November 2002 of monthly standardised outgoing long wave radiation (OLR) anomalies for the region from 5°N to 5°S, 160°E to 160°W, is shown in Fig. 2. These data were provided by the Climate Prediction Center, Washington D.C. (CPC 2002). Negative values of the OLR index suggest cooler black-body temperatures, which tend to be associated with an increase in high cloud and hence convection. (This may also signal increased rainfall.) Studies have shown that during El Niño events, convection is generally enhanced (i.e., reduced OLR) along the equator, whilst during La Niña events, convection is often suppressed (i.e., increased OLR) (Hoerling et al. (1997), Vincent et al. (1998)).

The OLR anomalies during the individual months of spring 2002 (−1.8, −1.3 and −1.4 for September, October and November respectively), together with the three-month moving average (Fig. 2), suggest greatly increased convection on the equator near the date-line. Furthermore, the raw values corresponded to near two standard deviations below the average during September and close to one and a half standard deviations below the normal during October and November. The November value, however, somewhat obscures the fact that OLR values dropped further during the latter half of the month.

The OLR anomaly for spring 2002 (Fig. 3) clearly shows enhanced convection along the equator, however during September and October the region of enhanced equatorial convection was in fact largely confined to within approximately 15° longitude of the date-line; further west than may ordinarily be expected during a warm ENSO phase. This westward shift in the OLR anomalies, and hence convection, may go some way to explaining the relatively weak values of the SOI. September OLR anomalies were particularly low, with values down to -55 W m^{-2} . November, however, saw enhanced convection along a greater stretch of the equator.

The values of the OLR anomalies were not only influenced by the underlying sea-surface temperature (SST) anomalies (see following section) but also by enhancement from active phases of the Madden Julian Oscillation (MJO) (Madden and Julian 1971, 1972). MJO active phases were apparent during August, which led to the substantially increased central equatorial convection (i.e., negative anomalies of OLR) which persisted through September. Another substantial MJO event in November was the cause of the late-month rally in the November convection. Once established, the enhanced convective regions maintained their presence for some time due to their modification of the low level winds (i.e., decreased

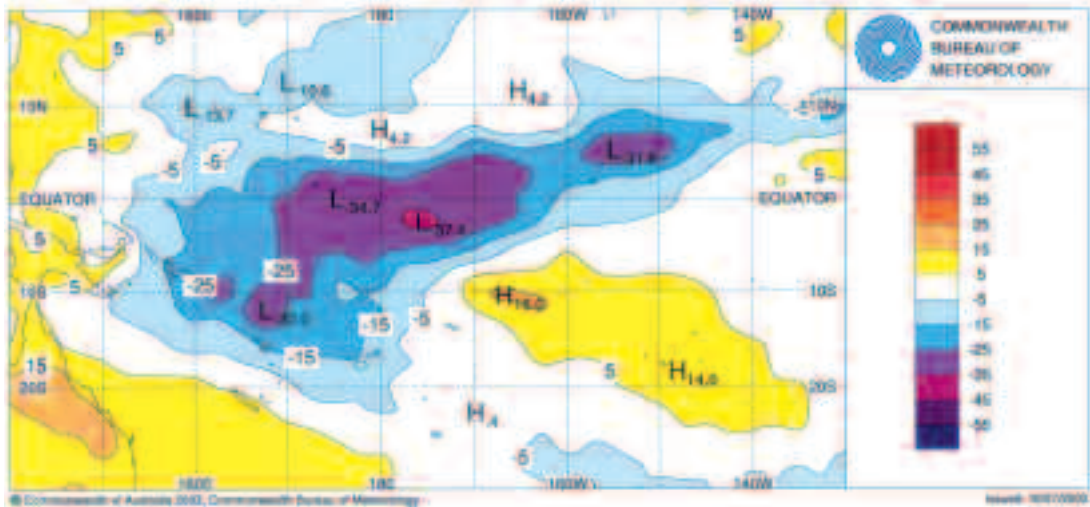
Fig. 2 Standardised anomaly of monthly outgoing longwave radiation averaged over 5°N-5°S and 160°E-160°W, for January 1998 to November 2002. Negative (positive) anomalies indicate enhanced (reduced) convection and rainfall. Anomalies are based on a 1979-95 base period. After CPC (2002).



strength of trades), and hence further reduction in the equatorial oceanic upwelling which enables the surface waters to remain warmer than they would ordinarily be.

The overall pattern of OLR for the South Pacific region was fairly typical of that expected during an El Niño event, despite the fact that the South Pacific convergence zone (SPCZ) was sometimes slightly southwest of its climatological position. (During El Niño events the SPCZ is ordinarily north and east of its average position (Vincent 1993).) Far below normal OLR (i.e., increased convection) existed in most regions near and along the equator, east of Papua New Guinea, whilst to a lesser extent decreased OLR also existed in the eastern South Pacific. Conversely, the western and southern South Pacific experienced above normal OLR (i.e., decreased high cloud). These conditions manifested themselves in the regional rainfall totals. In September, parts of Kiribati received over 1200 per cent of their normal monthly rains: highest values above normal were recorded in eastern Kiribati, with Kiritimati and Kanton Island recording 1488 per cent and 1220 per cent of their normal September rainfall (mean September rainfall, 36 and 27 mm respectively), a record high in both locations. Conversely, the southern and western Southwest Pacific region was dry. In the western Coral Sea, Willis Island recorded 15 consecutive months to October with rainfall below 75 per cent of the monthly average. Fiji reported very dry conditions in its southern and western regions during October, despite the continuation of strong southeasterly winds

Fig. 3. Anomalies of outgoing long wave radiation for spring 2002 ($W m^{-2}$), based on a base period of 1979-98.



which had affected the nation since June. In New Caledonia the period from September to November saw only 29 per cent of normal rainfall occur, while in the Papua New Guinea Western Highlands, drought affected crops were killed by damaging frosts (the result of little overnight cloud cover) in October. The dry conditions also brought wildfires to both New Caledonia and Indonesia, where thick smoke haze covered Sumatra and the Malaysian peninsula during October.

Ocean patterns

Sea-surface temperature (SST) patterns

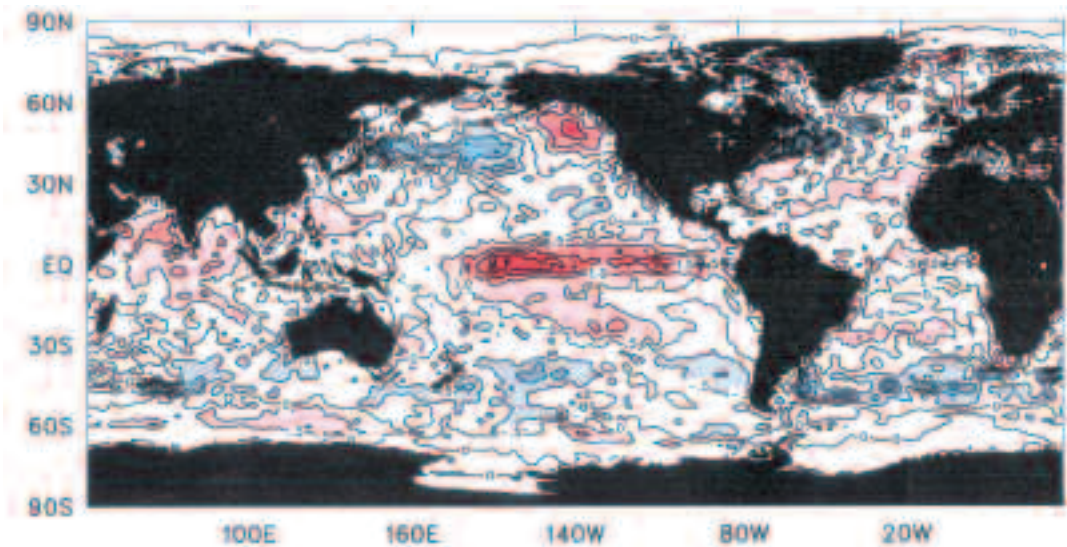
The mean spring 2002 SST anomaly distribution (Fig. 4) displayed positive anomalies (anomalies generally between $+0.5^{\circ}C$ and $+2.0^{\circ}C$) right along the equator from near $170^{\circ}E$ to the South American coast, with a further region of enhanced anomalies stretching diagonally across the South Pacific from western Kiribati to near southern French Polynesia.

The overall spring pattern hides the warming trend in both the equatorial and South Pacific regions that occurred throughout the season. In September, the main region with anomalies above $+1^{\circ}C$ existed between the date-line and $120^{\circ}W$, whilst in the South Pacific similarly warm anomalies only existed in the regions near French Polynesia. However oceanic downwelling Kelvin waves that crossed the equatorial Pacific during both September and October/November (see later discussion), resulted in

further warming of the subsurface. This enhanced warming was rapidly reflected in the SST values, resulting in anomalies of greater than $+2^{\circ}C$ in a broad region in the equatorial Pacific by mid-November. As a result, the November mean SST map showed values above $+1^{\circ}C$ from near $170^{\circ}E$ (Nauru) to the South American coast, in a band within approximately 5° latitude of the equator. Within this band, anomalies above $+2^{\circ}C$ occurred in several regions, including between the date-line and $140^{\circ}W$, as well as several smaller regions towards the South American coast. In the South Pacific, the November anomalies, largely driven by a strengthened, though slightly southwest of normal SPCZ, were above $+1^{\circ}C$ in a diagonal band across the region.

The strength of the November SST anomalies is highlighted by the fact that the full spring 2002 anomalies display a very similar pattern to the distribution for November alone, with only a reduction in the magnitude, clearly highlighting the warming trend during the season.

The increasing trend in the SST anomalies, as well as the tendency for the central equatorial Pacific to have anomalies somewhat greater than for regions closer to the South American coast, was made evident by the values for the various Nino indices. In the eastern equatorial Pacific, the Nino 1 and 2 values for September ranged from $-0.44^{\circ}C$ and $-0.06^{\circ}C$, respectively, to $+0.20^{\circ}C/+0.90^{\circ}C$ and then $+0.55^{\circ}C/+0.98^{\circ}C$ for October and November. Similarly, though with higher magnitude anomalies, in the central equatorial Pacific the Nino 3, 3.4 and 4

Fig. 4 Anomalies of sea-surface temperature for spring 2002 (°C).

values rose from $+0.83^{\circ}\text{C}/+1.25^{\circ}\text{C}/+1.01^{\circ}\text{C}$ in September to $+1.36^{\circ}\text{C}/+1.63^{\circ}\text{C}/+1.37^{\circ}\text{C}$ in November. (November standard deviations are $1.16^{\circ}\text{C}/1.14^{\circ}\text{C}/0.80^{\circ}\text{C}$.) The Niño 3 and 4 seasonal mean values of $+1.1^{\circ}\text{C}$ and $+1.2^{\circ}\text{C}$, respectively, were 0.5°C and 0.25°C above their wintertime values (Jones 2003). The Niño 1, 2, 3.4 and 4 indices all reached their peak values in November suggesting, at the surface, late November may have been the pinnacle of what was in a historical context, a relatively weak El Niño event.

In the mid to high latitudes, SST anomalies were generally negative with values 0.5 to 1.0°C below normal occurring between approximately 30°S and 50°S . This band of anomalous SST values was evident right around the globe, a response to the increase in the westerlies in this region (see Fig. 12) during the El Niño event. Such an increase in the westerlies, in a broad sense, is again a fairly typical response to a warm ENSO phase (Kwok and Comiso 2002). Low pressure at the low latitudes, by way of simple mass conservation, results in a strengthening of the subtropical ridge and hence increase in the mid latitude westerlies. Such an increase in wind strength may produce several impacts; an increase in surface mixing, an increase in the surface fluxes of heat and moisture, and an increase in the Ekman transport that draws cooler southern waters northwards. These factors may combine to lower the SST (as well as surface air temperature) in the region.

At the high latitudes, a number of regions are shown with positive SST anomalies, however values

were generally small. Composites from Kwok and Comiso (2002) suggest that at least in the regions off East Antarctica and north of the Amundsen and Bellingshausen seas, these patterns of warm anomalies are not unexpected during a warm phase of the Southern Oscillation.

However, it is worth noting that spring sees the time of maximum extent in the Antarctic sea ice pack (Watkins and Simmonds, 1999), and hence, in general, SST anomalies in the vicinity of the Antarctic coast are relatively meaningless (as they are ice covered), or very stable, as SSTs remain near constant at around -1.8°C (the freezing point of 35 per cent sea water).

At the outer edges of the sea ice pack (in the Austral spring in the vicinity of 60°S), the sea-ice concentration anomalies (not shown) were largely negative in the Amundsen, Bellingshausen and Ross seas (the Pacific sector), implying a lower concentration sea ice coverage than normal and hence a more southerly sea-ice edge. This was particularly so during November, which saw the outer pack sea-ice concentration, and hence the sea ice edge, considerably further south than the 1987-2001 baseline period. This region of maximum sea ice edge reduction, as well as the arguably greater sea ice edge increase in the vicinity of 15°E , corresponds remarkably with the Antarctic Dipole (ADP) pattern discussed by Yuan and Martinson (2001), whose dipole centres lay at 132°W and 24°E . This was despite the fact that they found the dipole pattern to be less apparent during El Niño than during La Niña events. (They suggest that

this is likely to be the result of the varying evolution of El Niño, as opposed to the more regular formation of La Niña, events. This has been shown for several other atmospheric circulation indices (Houseago et al., 1998.) The apparent excitement of the ADP by the warm ENSO conditions fits well with Yuan and Martinson's (2001) suggestion that the ADP and the Antarctic Circumpolar Wave (ACW) (White and Peterson 1996) are likely related, primarily due to the formation of the ADP by extra-polar processes during extreme ENSO phases, and the subsequent advection of the anomalies around Antarctica by the Antarctic Circumpolar Current.

In the Australian region, September to November 2002 SSTs were generally near normal, with slightly above normal SSTs off the east and northwest coasts, while slightly cooler than normal values were apparent off the southwest Western Australian and Tasmanian coasts. Interestingly, the pattern of SST anomalies of between +0.5 and +1°C off the Western Australian coast that had been apparent during autumn (Fawcett and Trewin 2003) and winter (Jones 2003), dissipated somewhat during spring, resulting in only weakly warm anomalies nearer the coast, though truly warm conditions remained in some form south of the Bay of Bengal.

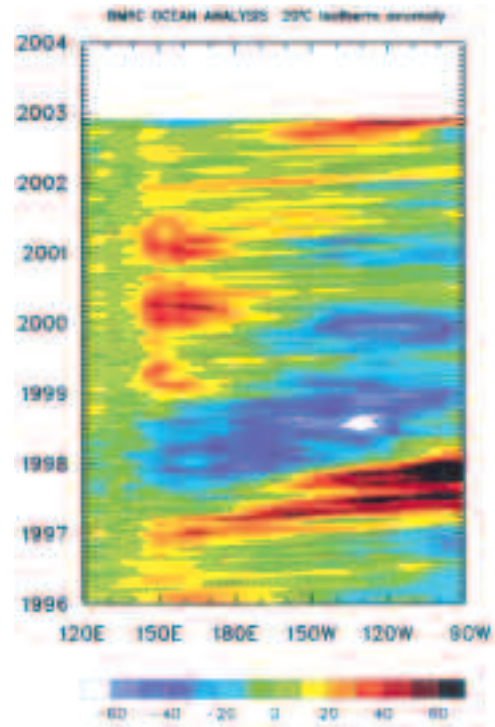
Subsurface ocean patterns

The Hovmöller diagram for the 20°C isotherm depth anomaly across the equator from January 1996 through to November 2002 is shown in Fig. 5. The 20°C isotherm depth is generally situated close to the equatorial ocean thermocline, the region of greatest temperature gradient with depth and the boundary between the warm near surface and cold deep ocean water. Changes in the thermocline depth may act as a precursor to future changes at the surface.

The El Niño event of 2002 truly commenced in June, after a downwelling oceanic Kelvin wave travelled across the equatorial Pacific during May, depressing the thermocline and hence allowing the increase in temperature of the subsurface waters (Jones 2003). This Kelvin wave was the result of an active phase of the MJO which initiated westerly wind bursts in the western Pacific.

As a result of the May oceanic Kelvin wave the equatorial subsurface warmed, and this was further enhanced/maintained by another such Kelvin wave in July and early August. Spring, however saw a further two Kelvin waves cross the equatorial Pacific (September and October/November), thus strengthening considerably the subsurface anomalies. As a result, 20°C isotherm anomalies of at least +20 metres were evident throughout spring everywhere east of the date-line, and anomalies reaching in excess of +40

Fig. 5 Time-longitude section of the monthly anomalous depth of the 20°C isotherm at the equator for January 1996 to November 2002. Base period: 1979-89. Contour interval is 10 m.



metres occurred in much of the eastern Pacific east of 140°W. In late November, local anomalies of +80 metres became apparent on the equator near 125°W which ultimately proved to be the peak of the 2002/03 El Niño event in the subsurface.

In the western equatorial Pacific (west of 170°E) the thermocline tended to be somewhat higher (i.e., negative 20°C isotherm anomalies), with values of -20 metres covering the region. Maximum magnitudes were reached during late October and early November when the thermocline was some 40 metres closer to the surface than normal.

The negative anomalies in the western equatorial Pacific were significant in two ways. Firstly, when combined with the strong depression of the thermocline in the eastern equatorial Pacific they produced the steepest west to east subsurface temperature anomaly gradient, and hence the 'flattest' east to west thermocline, of the 2002 El Niño event. This further highlights November as the peak of the El Niño in the Pacific Ocean. Secondly, and arguably more impor-

tantly in the longer term, they also signalled the onset of the upwelling oceanic Kelvin waves. Such upwelling oceanic Kelvin waves are the result of ENSO behaviour consistent with the 'delayed oscillator' theory of ENSO evolution and decay (Zebiak and Cane (1987); Suarez and Schopf (1988)) in which the initial (wind) forcing of the central Pacific triggers an eastward, equatorially trapped, downwelling oceanic Kelvin wave (as observed during May 2002 (Fawcett and Trewin 2003)) as well as an off-equator westward travelling upwelling oceanic Rossby wave. This Rossby wave later (theoretically around 4-5 months later; remarkably almost exactly the timing of the observed 2002 conditions) reflects off the western boundary and returns along the equator as an eastward travelling upwelling oceanic Kelvin wave. The upwelling oceanic Kelvin wave observed during late November did indeed herald the breakdown of the El Niño event in the subsurface, though it required a further upwelling Kelvin wave in December and January to fully seal the event's fate. The El Niño event of 2002/03, in the subsurface at least, was remarkably consistent in its timing and effect with delayed oscillator theory.

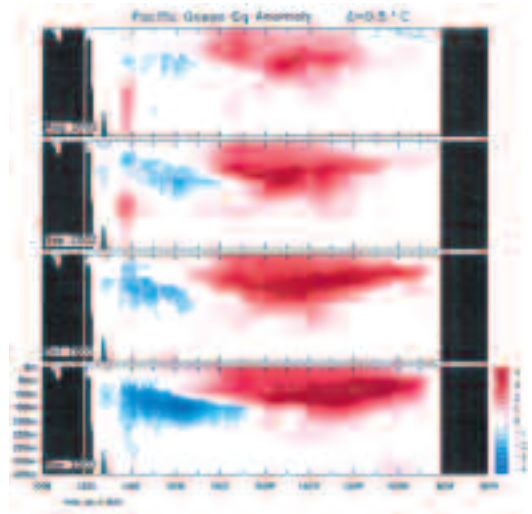
The cross-section of the equatorial Pacific temperature anomaly profile down to 400 metres for the months from August to November 2002 is presented in Fig. 6. This shows the progressive increase in subsurface temperature anomalies in the central to eastern Pacific, reaching over $+4^{\circ}\text{C}$ by November (maximum anomaly $+5.3^{\circ}\text{C}$), however in comparative terms this is far lower in magnitude than the anomalies observed at the peak of the previous El Niño event in 1997/98, when sub surface anomalies reached in excess of $+8^{\circ}\text{C}$ (not shown), thus supporting the description of the 2002/03 event as relatively 'weak'.

Comparisons of the equatorial subsurface to previous El Niño events shows a similar pattern of breakdown to that of 1994, with the intrusion of negative anomalies in the western equatorial Pacific during early spring that ultimately led to the breakdown of the event.

Surface analyses

The southern hemisphere spring 2002 mean sea-level pressure (MSLP) pattern, computed from the Australian Bureau of Meteorology's Global Assimilation and Prediction (GASP) model, is shown in Fig. 7, with the corresponding anomaly pattern provided in Fig. 8. These anomalies are the difference from an eleven-year (1979-89) climatology obtained from the European Centre for Medium Range Weather Forecasts (ECMWF).

Fig. 6 Four-month August to November 2002 sequence of vertical temperature anomalies at the equator. Contour interval is 0.5°C .



The spring MSLP pattern in Fig. 7 was largely zonal in structure, with arguably a wave number three pattern evident. Troughs were located at 30°E , 150°E and 120°W . As expected from climatology, the sub tropical ridge and the Antarctic high were the dominant features of higher pressure, whilst the Antarctic circumpolar trough was the significant feature of lower pressure.

The MSLP anomaly distribution (Fig. 8) for spring 2002 shows three distinct regions of note, all with at least some teleconnection to the low latitude warm ENSO event. In the tropical Pacific a widespread negative pressure anomaly existed east of the date-line with a maximum deviation from normal of -3.9 hPa . Such a reduction in pressure is clearly linked to the low level warming by enhanced SST values in the region (Fig. 4), and hence the shift in the Walker Circulation (Bjerknes 1969). This is also shown by the decrease (increase) in OLR (cloudiness) (Fig. 3).

The changes in temperature and pressure at the low latitudes also serve to drive the Hadley circulation with more vigour, resulting in a strengthening and southward movement of the sub tropical ridge, particularly in the southern Pacific region where anomalies were generally above normal though small in magnitude.

At the high latitudes, particularly in the Pacific sector, positive pressure anomalies of up to $+12.5\text{ hPa}$ were apparent. It has been shown that on both climatological (Simmonds and Budd 1991) and synoptic (Watkins and Simmonds 1995) time-scales, increased

Fig. 7 Mean sea-level pressure for spring 2002 (hPa).

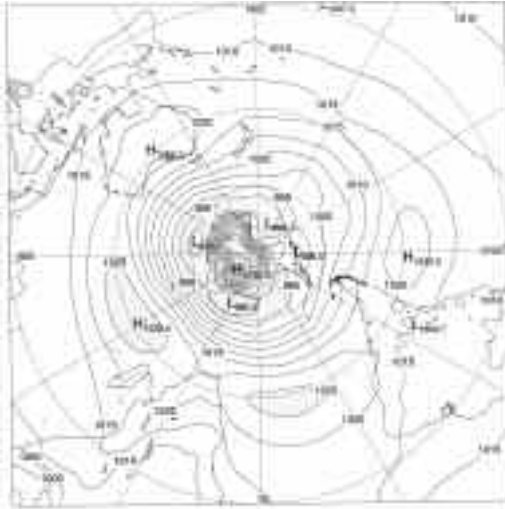
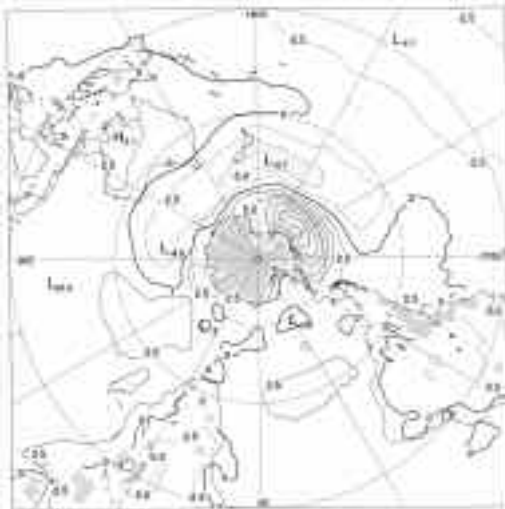


Fig. 8 Anomalies of the mean sea level pressure from the 1979-89 European Centre for Medium Range Weather Forecasts climatology, for spring 2002 (hPa).



sea-ice coverage may result in higher surface pressures through the effective separation of the relative warm ocean surface from the cool overlying atmosphere. However in this case there appears to have been, if anything, a decrease in sea ice concentration

in the Pacific sector implying that the above average pressures may have been related more to the southwards shift in the subtropical ridge and the strengthening of the westerlies than through purely local forcing. This out-of-phase relationship in the MSLP anomalies between the low and high latitudes has been recognised previously (see, for example, Mo and White (1985)).

Anomalies over the Antarctic are no longer shown, as MSLP values make little sense over a region averaging approximately 3500 metres elevation. This is further complicated by the extremely strong surface inversions making such anomalies difficult to interpret physically.

Over Australia the MSLP was far higher than normal with anomalies of up to +2.1 hPa over Western Australia. This pattern is again typical of that during an El Niño event, when an enhanced subtropical ridge tends to dominate the continent (Karoly 1989).

Mid-tropospheric analyses

The 500 hPa geopotential height (an indicator of the steering of surface synoptic systems) across the southern hemisphere is shown in Fig. 9, and anomalies in the 500 hPa field displayed in Fig. 10. Flow displayed a wave number four pattern. At the mid to high latitudes, the major 500 hPa height anomalies were centred over the same locations as their MSLP counterparts. Combined, this suggests a largely barotropic atmospheric structure.

In the low latitudes, however, the lower than normal surface pressure is only weakly reflected in the mid-troposphere, suggesting an atmospheric structure more baroclinic in nature. This is not surprising due to the enhanced atmospheric heating, the result of increased latent heat release into the troposphere from the greatly enhanced convection.

Blocking

The time-longitude section of the daily southern hemisphere blocking index (BI)* (Wright 1993) is shown in Fig. 11. This index is a measure of the strength of the zonal 500 hPa flow in mid latitudes relative to that at subtropical and high latitudes. Positive values of the blocking index are generally associated with a split in the mid-latitude westerly flow centred near 45°S and mid latitude blocking activity.

*BI=0.5[(u₂₅+u₃₀) - (u₄₀+2u₄₅+u₅₀) + (u₅₅+u₆₀)] where u_{xx} is the westerly component of the 500 hPa wind at latitude xx.

Fig. 9 Mean 500 hPa geopotential heights for spring 2002 (gpm).

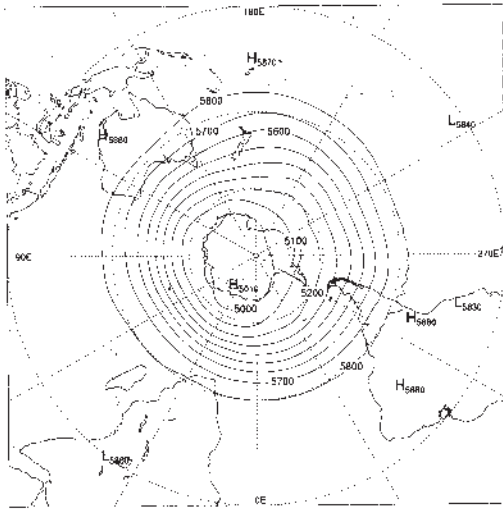
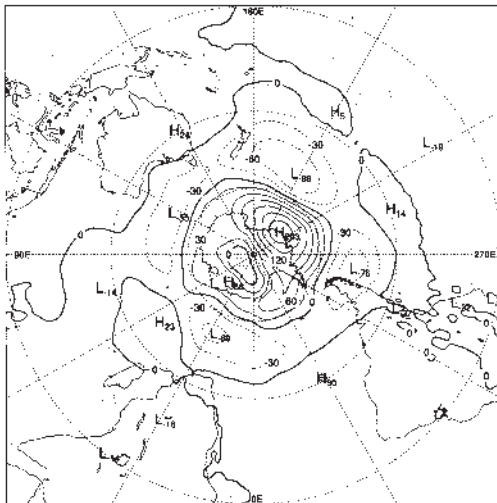


Fig. 10 Anomalies of the 500 hPa geopotential height from the 1979-89 European Centre for Medium-range Weather Forecasts climatology, for spring 2002 (gpm).



The BI values during spring 2002 showed remarkably few blocking events, with the first relatively strong block (BI > 60) not occurring until early October, though being only brief in duration. This occurred just on and east of the date-line. Of the five

(arguably six) other notable blocking events to occur during the season, only one occurred outside of this region. Once again this appears to be standard ENSO warm event behaviour, as Renwick (1998) showed an increase in blocking over the southeastern Pacific occurred during warm ENSO phases.

Mean blocking for the austral spring 2002 (Fig. 12) shows reduced values in all locations, a situation clearly representative of the increase in the mid-latitude westerlies associated with the peak of the El Niño event. The only region displaying mean positive values occurred between 170°E and 160°W, far narrower than the climatological mean positive BI region: 150°E to 120°W, or the region considered to be the climatologically favoured area for blocking systems; 140°E to 140°W (Trenberth and Mo 1985, Sinclair 1996).

Anticyclonicity (taken as the time in hours anticyclones spend in any 5°x5° sector: see Nowak and Leighton (1997)) maps for spring 2002 (not shown) indeed suggest that positive anticyclonicity anomalies in the Australian region were generally small (maximum anticyclonicity values of +48 hours) and centred near 32°S, with centres in the Great Australian Bight and in the northern Tasman Sea. This is to some degree a reflection of the positive MSLP anomalies over Australia (Fig. 8), which itself are related to the warm ENSO state, as well as the highly transient nature of the systems in the strengthened westerlies.

Elsewhere, in the Indian Ocean virtually no blocking occurred at all during the season, and only two blocks were evident in the South Atlantic.

Low and upper level winds

Spring 2002 low level (850 hPa) and upper level (200 hPa) wind anomalies (from the 11 year ECMWF climatology) are shown in Figs 13 and 14 respectively. The low level wind anomalies tended to reflect the MSLP anomalies observed over the corresponding period (Fig. 8), particularly in the middle to high latitudes, where they clearly display the low level increase in the westerlies in the mid latitudes and the strong increase in the easterlies closer to the Antarctic coast. The strongest increase in the mid-latitude westerlies occurred in the Pacific sector, between 150°E and 120°W.

In the tropical Pacific, low level winds reflected a weakening of the trades in those regions on or west of the main centre of anomalous convection (generally in the region near the date-line), as also observed during winter (Jones 2003). This is as expected during El Niño events (Larkin and Harrison 2002), as the low

Fig. 11 Spring 2002 daily blocking index: time-longitude section. Day 1 is 1 September.

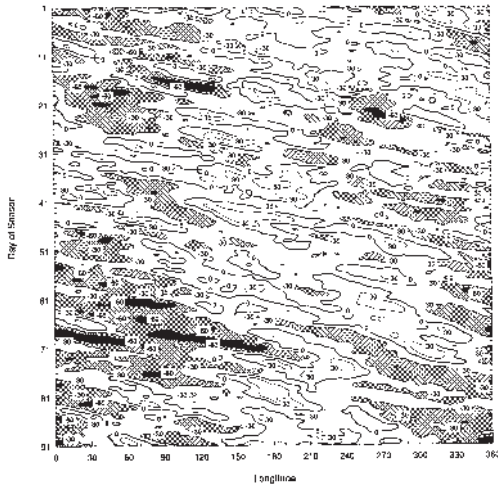
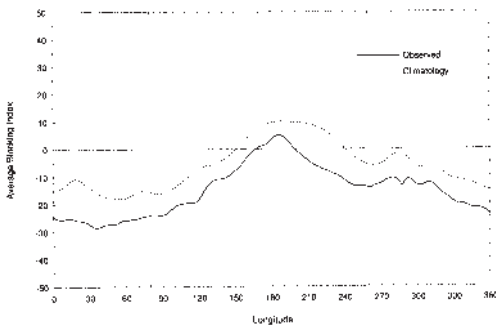


Fig. 12 Mean southern hemisphere blocking index for spring 2002 (bold line). The dashed line shows the corresponding long-term average. The horizontal axis shows the degrees east of the Greenwich meridian.

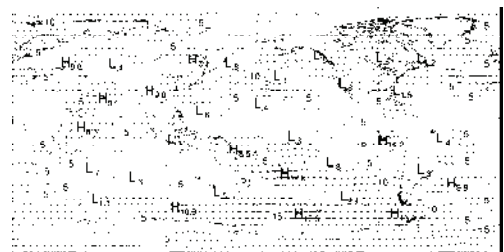


level convergence in the enhanced convective region draws in air from the surrounding regions. East of the convective area the trades tended to be enhanced slightly, again possibly due to the low level convergence which was particularly focused upon the date-line earlier in the season. These enhanced trades during spring 2002 east of the date-line (Fig. 13) occurred somewhat further west of the region where they might ordinarily be expected during a warm ENSO phase as shown by Larkin and Harrison (2002), however their pattern would appear consistent

Fig. 13. Spring 2002 850 hPa vector wind anomalies with contours of vector magnitude overlaid. The contour interval is 5 m s^{-1} , with values above 5 m s^{-1} stippled.



Fig. 14 Spring 2002 200 hPa vector wind anomalies with contours of vector magnitude overlaid. The contour interval is 5 m s^{-1} , with values above 5 m s^{-1} stippled.



with the westward lying OLR negative anomalies (Fig. 3). Upper level winds reflect the change in the Walker Circulation near the date-line with easterly anomalies on and near the equator.

The upper level wind anomalies (Fig. 14) over the southern hemisphere once again matched closely the theoretical atmospheric response to a warm ENSO phase (Karoly 1989) and continued the pattern first observed during the winter of 2002 (Jones 2003). As described by Jones (2003), in the Pacific sector an upper level region of anticyclonic anomaly lies to the south of the region of enhanced convection. The resulting north-south wavetrain (which curves somewhat to the east), is manifested by an upper level region of cyclonic anomalies near 45°S and an anticyclonic region to its south near 60°S . This wavetrain was remarkably similar to that shown schematically by Karoly (1989) during warm ENSO phases.

The anomalous anticyclone observed over Australia in winter (Jones 2003) remained apparent during the spring, with a clear anticyclonic circulation at the 850 hPa level. Easterlies over Cape York and the Top End were greatly enhanced, as were the westerlies to the south of the continent. Such circulation, once again, is a typical response of Australian region circulation to El Niño conditions in the equatorial Pacific (Jones and Simmonds 1994).

Ozone hole observations

The Austral spring is typically the time of the maximum extent of the Antarctic ozone hole, as well as the time of lowest annual ozone levels. In the absence of sunlight, the wintertime polar vortex in the lower stratosphere cools to below -80°C , and ice clouds form. Chlorine and bromine compounds react in the ice clouds to produce chemical species that, when combined with the incoming UV radiation as the sunlight returns in spring, destroy ozone (WMO 1998). As the stratosphere warms in spring (and hence ice clouds can no longer form) this process weakens. Ozone levels then return to near normal by early summer. The compounds that lead to the ozone breakdown are largely anthropogenic, but now appear to be in decline (WMO 1998).

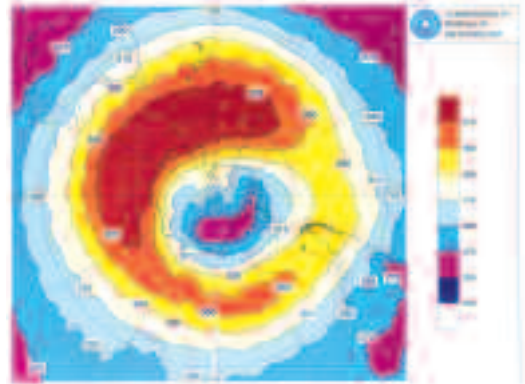
Figure 15 shows the mean ozone measurements for spring 2002 from the Total Ozone Mapping Spectrometer (TOMS) instruments. Typically, the ozone hole is taken as the area of total column ozone with a value of less than 220 Dobson units.

The Antarctic ozone hole during spring 2002 was arguably the most unusual observed in recent times (WMO 2002). Average areas of the ozone hole during September and October were smaller than in any year since 1988, peaking at around 19 million square kilometres on 20 September. This is considerably below the 1991–2002 mean peak value of well in excess of 21 million square kilometres, and far below that of the 2001 spring ozone hole maximum area of 25 million square kilometres.

Even more remarkable, however, was the separation of a large mass of air from the polar vortex in late September 2002 which resulted in the ozone hole splitting in two. In the last week of September this separated ozone hole dissipated and hence the total area of the hole dropped from its peak value to only 5 million square kilometres in the space of one week. Such a small area for the ozone hole in early October has not been observed since the early 1980's (WMO 2002).

The ozone hole was also unusually 'shallow', with a minimum total column ozone of about 135 Dobson Units (DU), considerably more than the 2001 value of

Fig. 15 Total column ozone values from the Total Ozone Mapping Spectrometer (TOMS) for Spring 2002 (Dobson Units).



closer to 100 DU and the record satellite observation of 88 DU in 1994. After the ozone hole split and reformed its minimum total column ozone was around 150 DU.

The final break-up of the 2002 spring ozone hole in the second week of November was also the earliest this has occurred since 1988.

It is important to note that the relatively weak nature of the 2002 ozone hole was a result of anomalous circulation and meteorological conditions associated with the polar vortex, and not an indication of a return to a normal chemical composition of the stratosphere.

Australian region

Rainfall

The distribution of Australian rainfall totals for spring 2002 is shown in Fig. 16, whilst Fig. 17 shows the associated decile ranges based on gridded rainfall data for all springs from 1900 to 2002. Australian rainfall patterns clearly reflected the widespread impact of the anomalously warm equatorial Pacific (Ropelewski and Halpert, 1987), with extremely dry conditions throughout virtually all of eastern Australia as well as large parts of the central and western mainland. The only regions to escape the spring drought conditions were in western Tasmania, which lay in the path of the stronger than usual westerlies, and parts of central and north-western Western Australia which typically have a weaker rainfall relationship with ENSO than most parts of the country (Ropelewski and Halpert 1987).

Fig. 16 Spring 2002 rainfall totals over Australia for spring 2002 (mm).

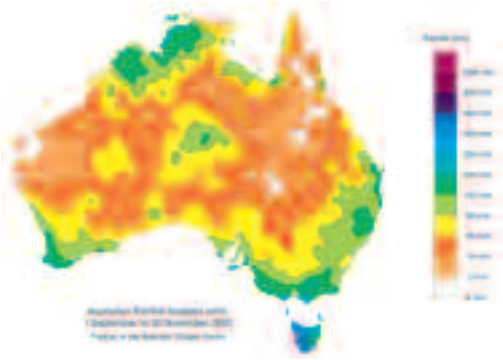
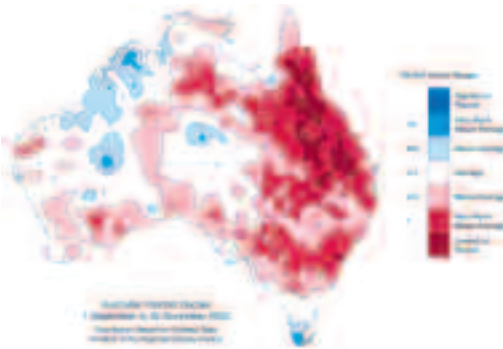


Fig 17 Spring 2002 rainfall deciles for Australia: decile range based on grid-point values over the spring periods from 1900 to 2002.



Highest rainfall totals for the season were recorded in western Tasmania, where in excess of 600 mm fell for the season. For the remainder of the continent, only very small pockets received rainfall in excess of 200 mm for the season, whilst rainfall in excess of 100 mm was confined to Tasmania, southern Victoria, south-western WA, eastern-most NSW and Queensland and the far north-west of WA. The driest regions occurred in the Gascoyne/Pilbara regions of WA, which is climatologically dry during spring, and through parts of central Queensland. In both of these regions there were areas which received less than 2 mm of rainfall for the season.

The extremely low spring 2002 rainfall deciles followed from equally low or lower values in winter (Jones 2003), when only Tasmania and the eastern half of Queensland were left unaffected. Unfortunately, however, spring brought dry condi-

tions to eastern Queensland as well, with many regions experiencing their lowest rainfall totals on record. The dry conditions of winter 2002 followed very dry conditions during autumn (Fawcett and Trewin 2003) when the northern half of the continent, as well as Tasmania, experienced very much below the average totals, with the remainder of the continent also below normal.

Overall, spring 2002 was the fifth driest spring, Australia-wide, on record (high quality rainfall records commence 1900) with a mean rainfall of only 39.7 mm for the season. This is only 4.3 mm above the lowest spring national-mean rainfall recorded (1967). The only years with a drier spring than 2002 are 1967, 1957, 1918 and 1944 (in order driest to least dry), of which 1957 and 1918 are also considered El Niño years. Spring 2002 saw 79 per cent of the area of the continent experience rainfall below the long term median, of which 26 per cent of the continent was in the lowest 10 per cent of recorded totals (i.e., decile 1). Furthermore, and as described above, this came on the heels of two seasons of equally low rainfall. Rainfall deficiencies for the full three season (autumn, winter, spring) period from March to November saw 98 per cent of the continent receive below median rainfall. Of this, 62 per cent of the total area of Australia experienced rainfall below the 10th percentile and there was a mean Australia-wide percentile value for the period of 11.

The low spring rainfall for the Australian region, while generally consistent with previous El Niño related droughts, was remarkably severe in magnitude given that anomalies in the equatorial Pacific were not considered equally extreme. However it is interesting to note that the previous El Niño related drought in Australia (1994) also had relatively weak oceanic anomalies, and that these anomalies were also located in the central/western equatorial Pacific, just as was the case in 2002. In contrast, the severe El Niño episode of 1997/98 that had relatively weak impacts upon Australian rainfall had its major oceanic anomalies in the central/eastern equatorial Pacific.

Temperatures

The spring 2002 mean maximum and minimum temperature anomalies, calculated with respect to the reference period 1961-90, are shown in Figs 18 and 19 respectively. Maximum temperature anomalies were strongly positive over virtually the entire continent with only very small and isolated coastal patches of anomalies of between 0 and -1°C . In general, anomalies of between $+1^{\circ}\text{C}$ and $+3^{\circ}\text{C}$ covered almost all of the western half of the continent, whilst the eastern half was even hotter, with anomalies ranging from $+1^{\circ}\text{C}$ to $+4^{\circ}\text{C}$ and a small region displayed anomalies

Fig. 18 Spring 2002 maximum temperature anomalies for Australia based on a 1961-90 mean ($^{\circ}\text{C}$).

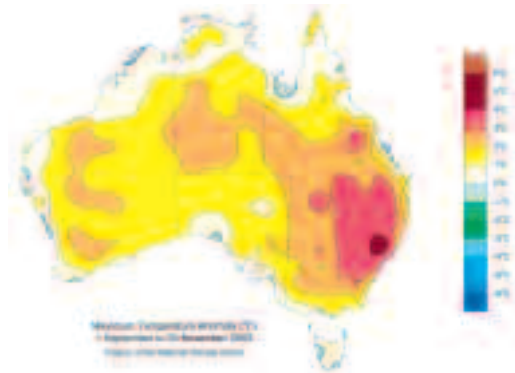
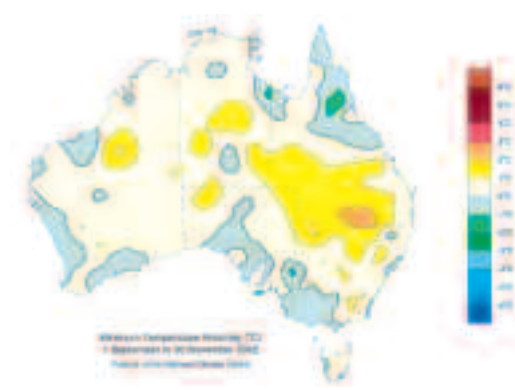


Fig. 19 Spring 2002 minimum temperature anomalies for Australia based on a 1961-90 mean ($^{\circ}\text{C}$).



of between $+4^{\circ}\text{C}$ and $+5^{\circ}\text{C}$. Minimum temperatures were closer to normal, with values over the continent generally in the range of -1°C to $+1^{\circ}\text{C}$, though a large region of $+1^{\circ}\text{C}$ to $+2^{\circ}\text{C}$ anomalies covered the southern half of Queensland.

Both the maximum and minimum temperature anomalies for spring were consistent with the general spatial impacts of an El Niño event upon Australian temperature (Jones and Trewin 2000), although the region of high minimum anomalies in southern Queensland occurred in an area which ordinarily has a weak correlation between the SOI and minimum temperature. Both the maximum and minimum temperatures reflect the strengthened subsidence and anticyclonic flow over the continent (Fig. 13) and reduced cloudiness. With little cloud there was a greater heat loss to space at night, greater radiation

reaching the surface during the day and reduced evaporative cooling (associated with the low rainfall).

However despite the patterns of maximum and minimum temperature anomaly being consistent with those that may be expected during a warm phase in the equatorial Pacific, the magnitudes of the anomalies were unheralded. The Australia-wide maximum temperature anomaly for spring was $+1.7^{\circ}\text{C}$, 0.3°C above the previous record set in 1980. (Seasonal Australia-wide temperature records commenced in 1950.) This follows on from record high maximum Australia-wide temperatures for both winter ($+1.4^{\circ}\text{C}$; previous record $+0.96$ (1996)) (Jones 2003) and autumn ($+1.8^{\circ}\text{C}$; previous record $+1.39^{\circ}\text{C}$ (1986)) (Fawcett and Trewin 2003). As a result, the three-season maximum temperature anomaly for March to November was $+1.65^{\circ}\text{C}$, massively surpassing the previous record of $+1.02^{\circ}\text{C}$ set in 1980 (Watkins 2002) and consistent with the warming trend observed in annual data since 1910. By contrast, minimum temperatures only showed an Australia-wide anomaly for spring of $+0.55^{\circ}\text{C}$, the 11th warmest on record. However, given the low cloud amounts over the continent and hence large night-time radiation loss to space this was warmer than may have been expected. It was also clearly warmer than the previous El Niño related droughts of 1982 and 1994, which experienced spring minimum temperature anomalies of -0.20°C and $+0.02^{\circ}\text{C}$, respectively.

Further highlighting the extremely high temperatures experienced during spring and through the entire El Niño period of 2002 were data for the Murray Darling Basin (MDB), which includes Australia's three longest rivers (Murray, Darling and Murrumbidgee), accounts for 41 per cent of the nation's gross value of agricultural production, and for 70 per cent of all water used for irrigation in Australia (Nicholls 2003). The MDB experienced a basin-wide mean maximum temperature anomaly of $+2.9^{\circ}\text{C}$ for spring, 0.6°C above the previous record maximum temperature. When such extreme temperature anomalies (and hence greatly increased evaporation) are combined with the MDB spring 2002 rainfall being the eighth driest out of 103 years (basin-wide mean spring 2002 rainfall of only 49 mm (1961-90 mean: 120 mm)) it becomes apparent why some questioned whether 2002 was the worst drought on record, and whether this may be linked to anthropogenic climate change. Nicholls (2003) showed that for the May to October 2002 period, temperatures in the MDB were considerably warmer than may have been expected given the low rainfall received, as well as far warmer than the previous El Niño related droughts in the region (1982 and 1994), and that this was part of a warming trend observed in the MDB since at least

1950. Nicholls (2003) suggests that even if rainfall totals do not change from one drought to the next, the possibility that the enhanced greenhouse effect is increasing the severity of Australian droughts by raising temperatures and hence increasing evaporation, needs to be considered.

Appendix

The main sources for data used in this review were:

- National Climate Centre, *Climate Monitoring Bulletin - Australia*. Obtainable from: National Climate Centre, Bureau of Meteorology, GPO Box 1289K, Melbourne, Vic., 3001, Australia.
- Climate Prediction Center, *Climate Diagnostics Bulletin*. Obtainable from: Climate Prediction Center, National Weather Service, Washington D.C., U.S.A., 20233.
- World Meteorological Organization, *Antarctic Ozone Bulletin*. Obtainable from: <http://www.wmo.ch/web/arep/gawozobull02.html>

References

- Bjerknes, J., 1969. Atmospheric teleconnections from the equatorial Pacific. *Mon. Weath. Rev.*, 97, 163-72.
- Climate Prediction Center (CPC) 1999. *Climate Diagnostics Bulletin*, September, October and November 2002. U.S., Dept. Of Commerce, National Oceanic and Atmospheric Administration, Washington D.C., USA.
- Fawcett, R.J.B. and Trewin, B.C. 2003. Seasonal climate summary southern hemisphere (autumn 2002): onset of El Niño conditions. *Aust. Met. Mag.*, 52, 127-36.
- Hoerling, M.P., Kumar, A. and Zhong, M. 1997. El Niño, La Niña, and the nonlinearity of their teleconnections. *Jnl climate*, 10, 1769-86.
- Houseago, R., McGregor, G., King, J.C. and Harangozo, S.A. 1998. Climate anomaly wave-train patterns linking southern low and high latitudes during South Pacific warm and cold events. *Int. J. Climatol.*, 18, 1181-93
- Jones, D.A. 2003. Seasonal climate summary for the southern hemisphere (winter 2002): consolidation of El Niño conditions in the Pacific. *Aust. Met. Mag.*, 52, 203-12.
- Jones, D.A. and Simmonds, I. 1994. A climatology of southern hemisphere anticyclones. *Clim. Dyn.*, 10, 333-48.
- Jones, D.A. and Trewin, B.C., 2000. On the relationships between the El Niño-Southern Oscillation and the Australian land surface temperature. *Int. J. Climatol.*, 20, 697-719.
- Karoly, D.J. 1989. Southern hemisphere circulation features associated with ENSO events. *Jnl climate*, 2, 1239-52.
- Kwok, R. and Comiso, J.C., 2002. Southern Ocean climate and sea ice anomalies associated with the Southern Oscillation. *Jnl climate*, 15, 487-501
- Larkin, N.K. and Harrison D.E., 2002. ENSO warm (El Niño) and cold (La Niña) event life cycles: ocean surface anomaly patterns, their symmetries, asymmetries, and implications. *Jnl climate*, 15, 1118-40
- Madden, R.A. and Julian, P.R. 1971. Detection of a 40-50 day oscillation in the zonal wind in the tropical Pacific. *J. Atmos. Sci.*, 28, 702-8.
- Madden, R.A. and Julian, P.R. 1972. Description of global scale circulation cells in the tropics with a 40-50 day period. *J. Atmos. Sci.*, 29, 1109-23.
- Mo, K.C. and White, G.H., 1985. Teleconnections in the southern hemisphere. *Mon. Weath. Rev.*, 113 22-37.
- Nicholls, N. 2003. The changing nature of Australian droughts. *Climatic Change* (in press).
- Nowak, H. and Leighton, R.M., 1997. Relationships between east coast Australasian anticyclonicity, the Southern Oscillation and Australian rainfall. *Aust. Met. Mag.*, 46, 267-76.
- Renwick, J.A. 1998. ENSO-related variability in the frequency of South Pacific blocking. *Mon. Weath. Rev.*, 126, 3117-123.
- Ropelewski, C. F. and Halpert, M. S., Global and regional scale precipitation patterns associated with the El Niño/Southern Oscillation. *Mon. Weath. Rev.*, 115, 1606-26.
- Simmonds, I. and Budd, W.F. 1991. Sensitivity of the southern hemisphere circulation to leads in the Antarctic pack ice. *Q. Jl R. Met. Soc.*, 117, 1003-24.
- Sinclair, M.R. 1996. A climatology of anticyclones and blocking for the southern hemisphere. *Mon. Weath. Rev.*, 124, 245-63.
- Suarez M.J. and Schopf, P.S. 1988. A delayed action oscillator for ENSO. *J. Atmos. Sci.*, 45, 3283-7.
- Trenberth, K. and Mo, K.C. 1985. Blocking in the southern hemisphere. *Mon. Weath. Rev.*, 113, 3-21.
- Vincent, D.G. 1993. The South Pacific Convergence Zone (SPCZ): a review. *Mon. Weath. Rev.*, 122, 1949-70.
- Vincent D.G., Fink, A., Schrage, J.M. and Speth, P. 1998. High- and low-frequency intraseasonal variance of OLR on annual and ENSO timescales. *Jnl climate*, 11, 968-86.
- Watkins, A.B. 2002. 2002 Australian climate summary: dry and warm conditions dominate. *Bull. Aust. Met. Ocean. Soc.*, 15, 109-14.
- Watkins, A.B. and Simmonds, I. 1995. Sensitivity of numerical prognoses to Antarctic sea ice distribution. *J. geophys. Res.*, 100, 22681-96.
- Watkins, A.B. and Simmonds, I. 1999. A late spring surge in the open water of the Antarctic sea ice pack. *Geophys. Res. Lett.*, 26, 1481-4.
- White, B. W. and Peterson, R. G. 1996. An Antarctic circumpolar wave in surface pressure, wind temperature and sea ice extent. *Nature*, 380, 699-702.
- Wolter, K. and Timlin, M. S. 1993. Monitoring ENSO in COADS with a seasonally adjusted principal component index. *Proc. of the 17th Climate Diagnostics Workshop*, Norman, OK, NOAA/NMC/CAC, NSSL, Oklahoma Clim. Survey, CIMMS and the School of Meteor., Univ. of Oklahoma, 52-57.
- Wolter, K. and Timlin, M. S. 1998: Measuring the strength of ENSO - how does 1997/98 rank? *Weather*, 53, 315-24.
- World Meteorological Organization (WMO) 1998. Scientific assessment of ozone depletion: 1998. *Global Ozone Research and Monitoring Project Report No. 44*, WMO, Geneva. 500pp.
- World Meteorological Organization (WMO) 2002. *WMO Antarctic Ozone Bulletins*. [Available from: <http://www.wmo.ch/web/arep/gawozobull02.html>]
- Wright, W.J. 1993. Seasonal climate summary southern hemisphere (autumn 1992): signs of a weakening ENSO event. *Aust. Met. Mag.*, 42, 191-98.
- Yuan, X. and Martinson, D.G. 2001. The Antarctic Dipole and its predictability. *Geophys. Res. Lett.*, 18, 3609-12.
- Zebiak, S.E. and Cane, M.A. 1987. A model El Niño -Southern Oscillation. *Mon. Weath. Rev.*, 115, 2262-78.